LA-UR--91-1687

DE91 013688

TITLE: Neutron Diffraction Determination of Residual Stress Redistribution in Cracked Autofrettaged Tubing

AUTHOR(S): M. A. Bourke, Los Alamos National Laboratory
H. J. McGillivray, Imperial College, London, U.K.
G. A. Webster, Imperial College, London, U.K.
P. J. Webster, Salford University, Salford, U.K.

SUBMITTED TO: Proceedings of the NATO Advanced Workshop on Measurement of Residual and Applied Stress Using Neutron Diffraction

DISCLAIMER

Los Alamos National Laboratory
Los Alamos, New Mexico 87545

NEUTRON DIFFRACTION DETERMINATION OF THE RESIDUAL STRESS REDISTRIBUTION IN CRACKED AUTOFRETTAGED TUBING

M.A.M. Bourke†, H.J. McGillivray*, G.A.Webster* & P.J. Webster◊

† LANSCE, Los Alamos National Laboratory, Los Alamos, NM, 87545, USA

* Dept of Mech Eng. Imperial College, Exhibition Rd London SW7 2BX

◊ Dept of Civil Engineering, Salford University, Salford, M54WT

Abstract. Neutron diffraction has been used to measure the residual stress distributions in uncracked and fatigue cracked rings taken from a high strength, low alloy steel autofrettaged tube with a bore diameter of 60mm and a wall thickness of 32mm. Stresses were determined to a precision of ± 10MPa. Three crack sizes were examined. No appreciable stress redistribution was observed until the crack was grown into a region which originally contained tensile residual hoop stress. When this occured an increase in residual hoop tension was observed ahead of the crack tip. Qualitative agreement was achieved between the measured hoop stress distribution and values predicted using a boundary element method.

1. Introduction

Thick walled tubing is used in a variety of high pressure, military and chemical engineering applications. When subject to cyclic internal pressure, fatigue cracks can propagate from the bore of the tube and cause failure. The autofrettage process, which is applied prior to service, provides some protection against fatigue cracking from the bore by applying internal pressure of sufficient magnitude to cause partial yield through the wall thickness. This introduces a compressive residual hoop stress at the bore which is balanced by a tensile stress at larger radii. The magnitude of the over-pressure determines the limit of the plastic zone and the shape of the stress distribution through the wall. Subsequent applied loading must first overcome the compressive residual hoop stress before cracks can propagate from the bore. The benefits of autofrettage in improving the fatigue life of tubing are documented elsewhere [1].

The stress produced by autofrettage in uncracked autofrettaged specimens has already been measured both by neutron diffraction and conventional methods [2]. In this study we have examined the redistribution of residual stress resulting from the growth of fatigue cracks from the bore. The effects of different crack lengths corresponding to different fractions of the wall thickness were studied. While the crack remains in the compressive region little redistribution was expected since the crack plane can still transmit a compressive force. However, when the crack traverses a region which originally contained a tensile stress, redistribution must occur since the cracked region can no longer transmit a tensile load.

2. Specimens

Thick walled tube of internal diameter 60mm and external diameter 124mm (diameter ratio 2.07) was subjected to an internal pressure of 662MPa. The bore is defined as R=0 and the outer edge as R=32mm. Yielding through 40% of the 32mm wall thickness was expected. The tube material was a high strength, low alloy steel containing

principal alloying additions of 0.34%C, 1.67%Ni and 0.8%Cr (AISI 4333M4). The autofrettage was applied without producing end loading on the tube and corresponded to plane stress. The yield stress was 1070MPa and the U.T.S. was 1150MPa.

Rings of thickness 5mm were removed from the tube after autofrettage (fig 1). Previous studies suggest that the removal of thin rings from autofrettaged tubing does not substantially alter the residual hoop stresses [3]. Although it is worth noting that finite element analyses of thin walled tubing do indicate a significant reduction in the hoop stress on removal of thin slices [4]. In practice the 5mm thickness of the specimens was selected to give fast count times thus making efficient use of the neutron beam time available. A 2.5mm deep notch was introduced at the bore of three rings from which fatigue cracks 4.5, 8.5 and 16mm in length (including the notch) were propagated. The crack lengths corresponded to failure through ≈14%, 25% and 50% of the wall thickness respectively. Previous measurements indicated that the change from compression to tension occurs approximately 8mm from the bore [2]. Relative to the original hoop stress distribution the crack tips lie in the compressive region, 0.5mm into the tensile region and 8mm into the tensile region (fig 2).

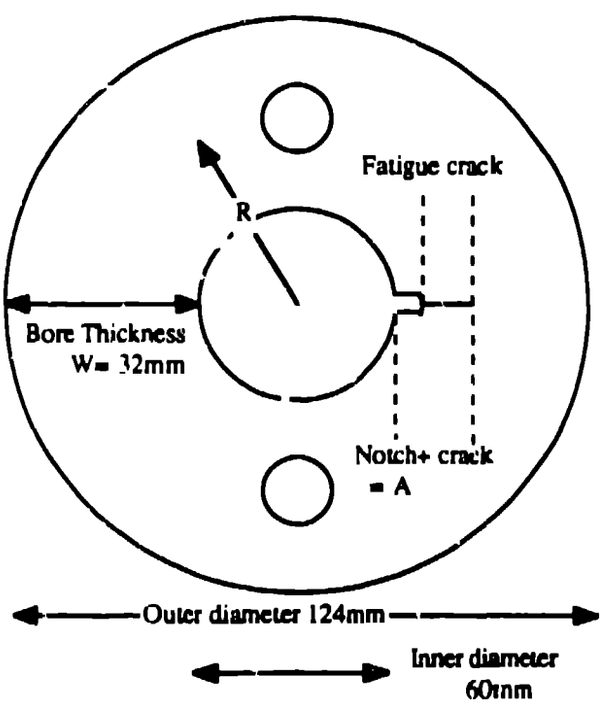

Figure 1 Dimensions of AF ring

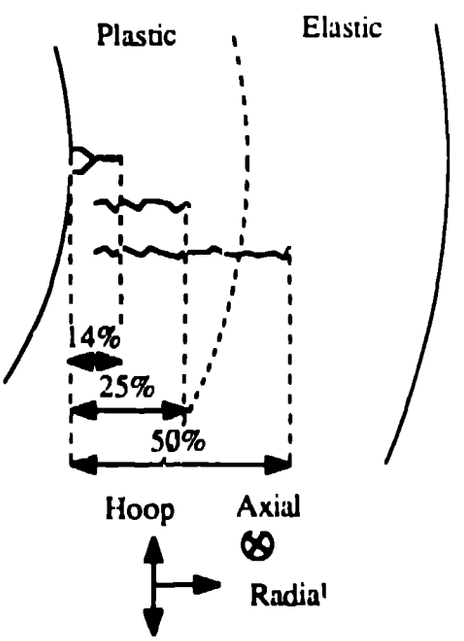

Figure 2: Crack lengths

3. Experimental measurements

The neutron diffraction technique uses the interplanar lattice spacings of selected Bragg reflections to act as internal strain gauges and is described elsewhere [5]. The measurements were made using the high flux research reactor at the Institut Laue Langevin, in Grenoble, France. Strains were determined by measuring the ferritic 211 reflection using the high resolution powder diffractometer, D1A which fell at an angle of ≈109.5°2θ for a wavelength of ≈1.91Å. The 211 reflection was selected because it has a

single crystal compliance close to the bulk macroscopic response. Count times were typically 20 minutes for each measurement giving an accuracy of ±40μstrain.

The presence of a crack disrupts the circular symmetry of the stress distribution produced by the autofrettage process. Consequently a compact sampling volume was required to resolve changes along the crack plane. A sampling volume of $8mm^3$ was used for all measurements and was placed on the centre plane at mid-thickness. Hoop, radial and axial strains were measured on a radius from the notch to the outside edge and along the opposite uncracked radius.

Strains are determined from the change in position of a measured Bragg reflection from the position of a reflection from unstrained material. The unstrained response is normally measured on material which is identical in composition to the specimen but which is small enough to be assumed to be free of significant macroscopic stress. However in this case the unstrained value was calculated by assuming that the forces acting across the plane of the uncracked side must balance. A moment balance is also possible and the stresses from the two methods of obtaining the unstrained response differ by less than 10MPa.

4.1 Results

Uncracked side (fig 3abc, fig 5): The strains and stresses for the uncracked sides of the three rings show that even when the fatigue crack is half way through the bore on one side of a ring no detectable redistribution of stress occurs on the uncracked side. Within experimental accuracy the stresses on the uncracked side were the same as previous measurements in an uncracked ring [2]. The unmodified autofrettage hoop stress shows a maximum compressive value at the bore of -300MPa reducing to zero at R=7.5mm then attaining a maximum tensile value of ≈80MPa at R=10mm (fig 5). The radial and axial stresses remain within ± 50MPa of zero at all points through the wall thickness. The radial stresses for all three rings approach zero at the bore and at the outer edge as they must at free surfaces.

Cracked side hoop direction (figs 4a,6a): The hoop strains (fig 4a) along the shortest, 4.5mm crack are close to the uncracked values (fig 3a). The maximum disparity of ≈20% occurs at R=2.5mm which corresponds to the depth of the notch. However the disparity between the uncracked and cracked results diminishes away from the notch and the change from compressive to tensile strain coincides at R≈7.5mm.

The hoop strains along the longest (16mm) crack demonstrate a characteristic shoulder between R=6 and R=14mm along which the strain is approximately constant and compressive. Beyond R=14mm the hoop strain becomes increasingly tensile to a maximum of 1400 μstrain between R=16 and R=17mm. The compressive shoulder is ≈-80MPa and a maximum tensile stress of 300MPa is reached at R=17mm (fig 6a).

The hoop strain along the crack plane of the intermediate crack length (8.5mm) hints at a similar shoulder to that described above at R=6mm. It also showed an increase in tension beyond the crack tip which was less than was observed for the longest crack length but exceeds the uncracked ring response.

Cracked side radial direction (figs 4b, 6b): On the cracked side the radial strains do not show consistent behaviour and in particular the results for the shortest crack are clearly in error (fig 6b). The stresses at the bore are not zero but this may reflect the presence of the notch. At the outer edge the radial stress for the intermediate and long crack rings do approach zero but not the shortest crack which reflects the anomaly described above.

Cracked side axial direction (figs 4c, 6c): Along the crack plane the axial strains are a tensile along the cracked region. Then at each crack tip there is a sharp discontinuity

to compressive strain along the remaining ligament. The discontinuity is not well defined for the shortest crack length which may reflect poor spatial resolution for those measurements.

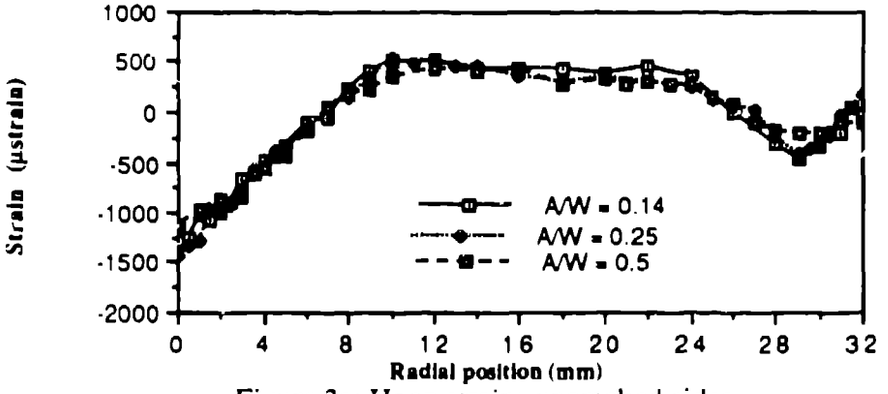

Figure 3a: Hoop strains uncracked sides

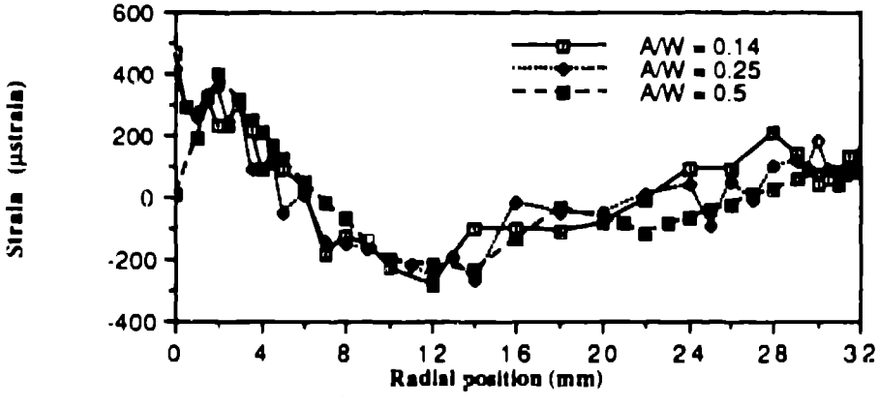

Figure 3b: Radial strain uncracked sides

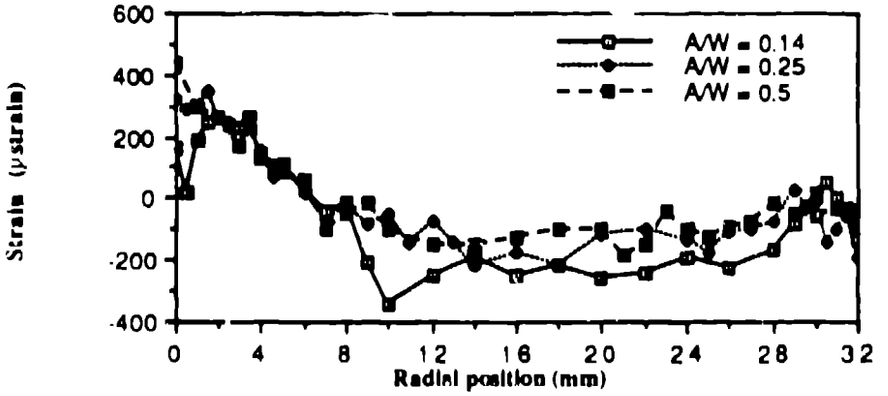

Figure 3c: Axial strain uncracked sides

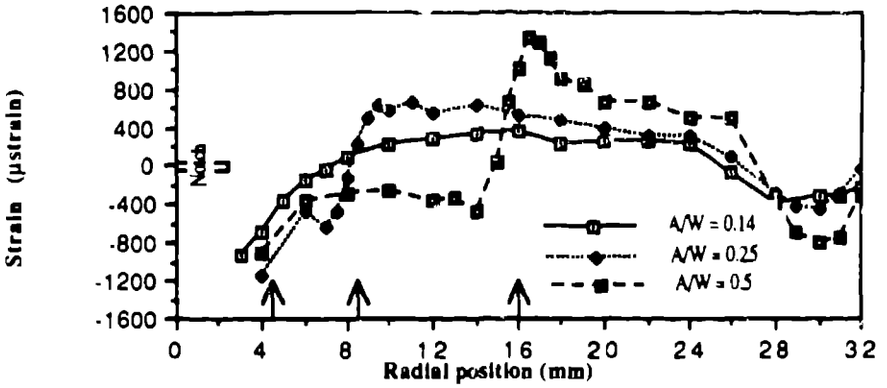

Figure 4a: Hoop strain uncracked sides

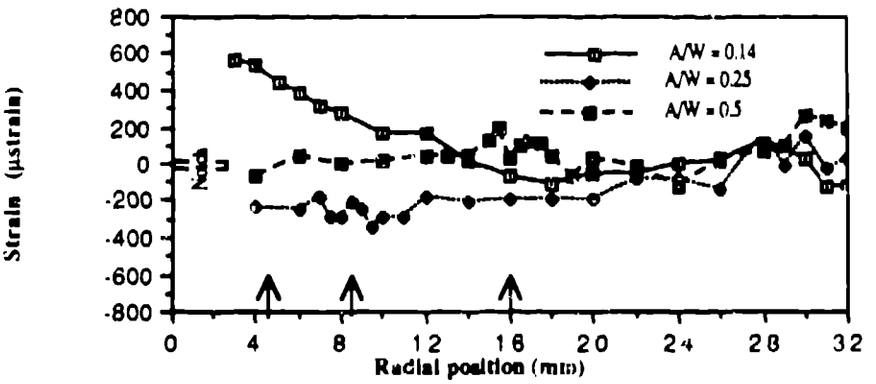

Figure 4b: Radial strain uncracked sides

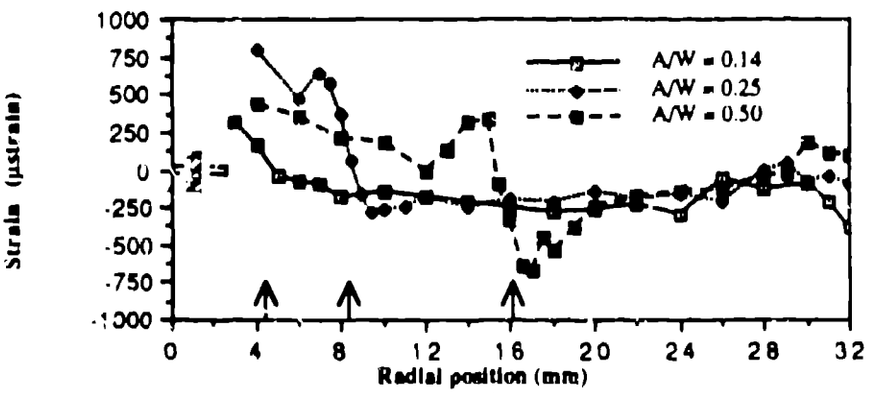

Figure 4c: Axial strain uncracked sides

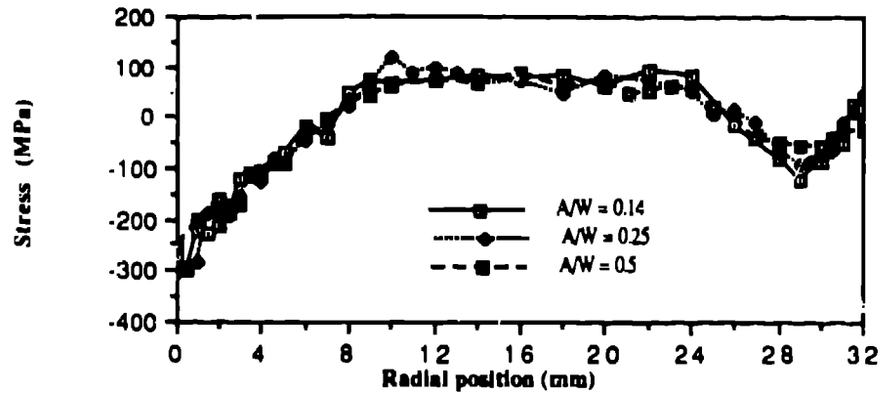

Figure 5: Hoop stress uncracked sides

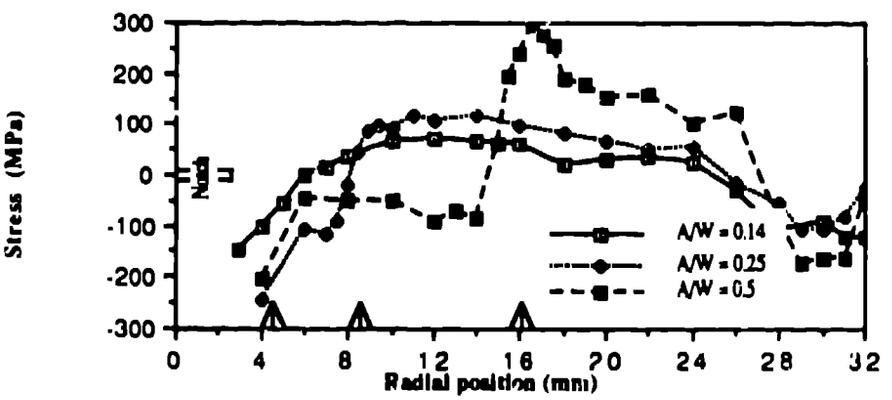

Figure 6a: Hoop stress cracked sides

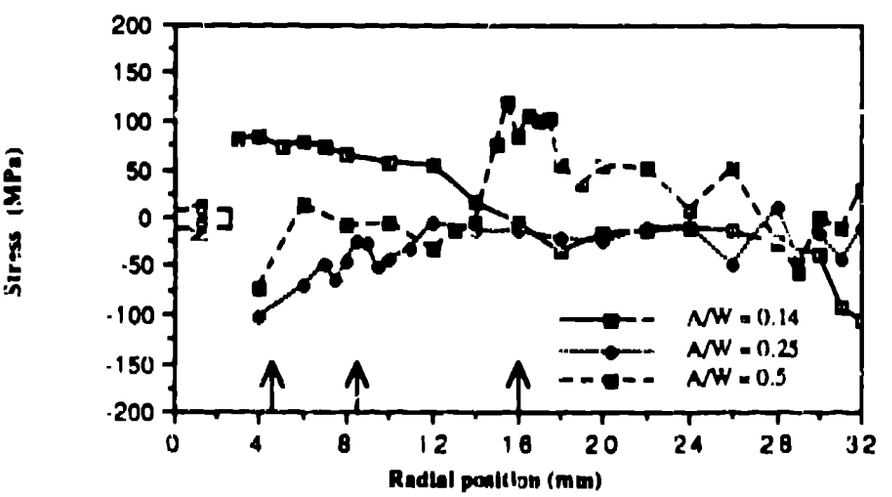

Figure 6b: Radial stress cracked sides

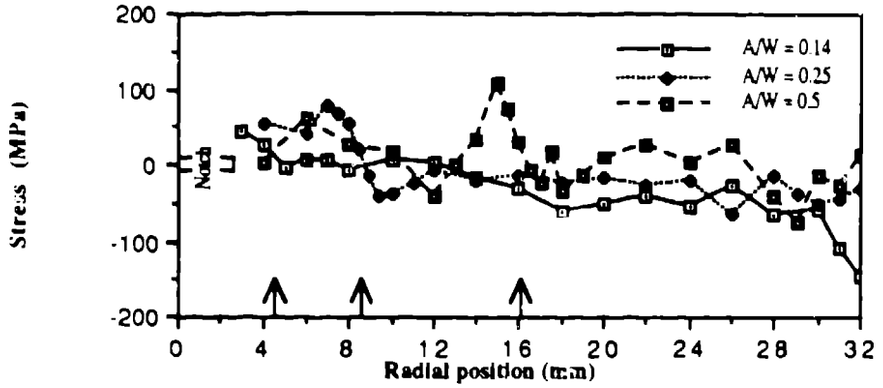

Figure 6c: Axial stress cracked sides

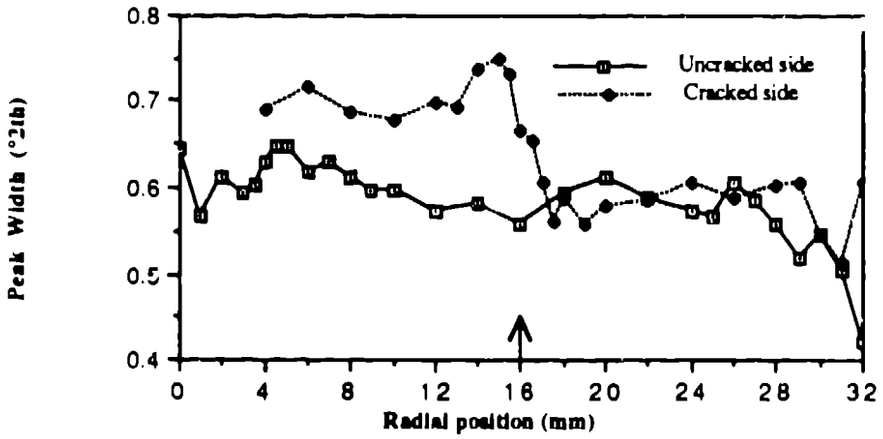

Figure 7: Peak widths axial strain (A/W = 0.5)

4.2 Comments on results

Along the crack planes the hoop and axial strains show consistent changes but the radial strains do not form a pattern. The hoop and axial strains on the cracked side of the shortest crack are close to the uncracked values thus the same was expected of the radial strain. This was clearly not the case. We believe that poor spatial resolution for those measurements may explain the discrepancy.

In figure 6a the hoop stress changes from compressive to tensile between R=14 and R=15mm which is closer to the bore than the visual identification of the crack tip at 16mm. Since a crack cannot support a tensile stress across it, either the positioning or the visual identification of the crack tip position is in error. The intensity profiles of the Bragg reflection as the sampling volume emerged from the specimen indicated that its position was correctly known. Thus it is believed that the crack tip is less than 16mm from the bore.

One interesting feature concerned the width of the Bragg reflections. In principle the shape and width of the diffracted peaks can provide information about the plastic

deformation and microstrain present in the material although care must be taken to separate broadening effects due to the finite sampling volume in regions of steep stress gradients. Comparison of data from the cracked and uncracked sides showed an increase in the width of the Bragg reflections in the vicinity of the fatigue crack this effect is illustrated for the axial strain direction of the longest crack in figure 7. Similar results were noted in the hoop and radial directions. On the uncracked side of each ring there is an approximate 16% reduction in the width of the diffracted peaks from the bore to the outer edge. On the cracked sides there is a further increase in width associated with the presence or passage of the fatigue crack. The effect is independent of the stress gradients which also alter the peak width. No quantitative use has been made of this information.

5.1 Boundary integral method

The boundary integral equation (BIE) or boundary element method is a stress analysis tool which provides solutions to engineering problems for which no analytical solution is available. It is a numerical technique which converts the partial differential equations which describe the elastic behaviour of a material to a surface integral applicable over a boundary. The conversion is exact and approximation is only introduced by the subsequent numerical solution of the integral. By applying tractions and displacements to points on a boundary the distribution of tractions and displacements at other points on the boundary can be predicted subject to any enforced conditions.

Boundary element methods combine known solutions of simple problems to give solutions to more complicated problems. If a force of known direction and magnitude acts at a point on the boundary of a material then subject to the laws of elasticity an analytical solution exists for the forces and displacements which act on any other point. By considering the application of multiple individual forces the fundamental solution associated with each can be superposed and by applying boundary conditions the effective traction and displacement over the remainder of the boundary can be predicted. Application of boundary integral methods to stress analysis is discussed by Fenner [6] and has been applied for calculating stress intensity factors in autofrettaged rings [7].

Unlike finite element methods in which the whole of the relevant domain must be discretised only the boundary is considered. This simplifies the model and reduces the dimensionality of the problem by one. Fewer elements are needed than equivalent finite element models which reduces the preparation and computing time. No approximation of the internal region is necessary which improves accuracy and produces less unwanted information. Selection of an appropriate mesh makes it easier to focus on a region of interest. Cracks can be introduced by creating new boundaries which can be external or internal.

Within each element on the boundary the displacement and tractions are described by nodal values together with a shape function for interpolation. Integrations along the boundary can be complicated and the solution is usually effected using Gaussian quadrature applied to the boundary elements. Small strains are implicit otherwise the shape of the domain will be altered.

5.2 Application of boundary integration

The features in the cracked rings which are open to modeling using the boundary element method are the notch (which initiates the fatigue crack) and the presence of a crack in the tensile region. Removal of material to form a notch permits the faces to compress in response to the residual stress at the bore and thus no compressive load is transmitted between R=0 and R=2.5mm. Similarly when the crack has propagated beyond 25% of

the wall thickness it relieves the tensile hoop stress because the cracked region cannot transmit a tensile force. In the tensile region the crack is drawn open and the stress must redistribute. For the rings containing the short and intermediate crack lengths all or most of the crack lies in the compressive region and the modification to the stress distributions is limited to the presence of the notch. Consequently the boundary element method was addressed to the ring containing the longest crack in which approximately 8mm of the original tensile hoop stress between R=~.5 and R=16mm is relieved.

A boundary element program [8] was used for the calculations. The program assumes plane strain conditions and uses Hermitian cubic elements. Cubic variations of displacements and tractions are permitted along each element. In figure 8 the original autofrettaged hoop stress distribution is illustrated across the wall of a ring. In figure 9 the position of the crack tip is indicated and the shaded regions AB and CD denote the relieved regions corresponding to the notch and to the region of the ring where the crack lies in an originally tensile stress region.

The BIE program was used to predict the stresses induced in the regions BC and DE for an applied stress distribution corresponding to the shaded regions in figure 9. Assuming superposition and adding the original hoop stress distribution (fig 8) to the predicted stress distribution due to the applied stresses in (fig 9) the stresses in the region AB and CD are negated. The modified stresses in regions BC and DE are then the residual stresses of interest.

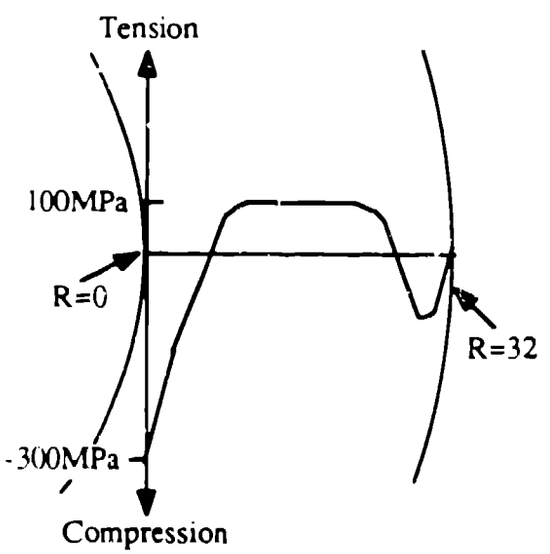

Figure 8: Original AF hoop stress

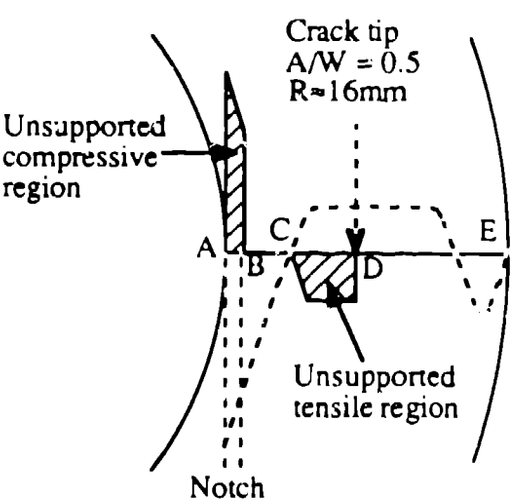

Figure 9: Applied stress for BIE calculation

Symmetry requires that only half of the ring needs to be modeled. The mesh used for the calculations is shown in figure 10. 58 nodes were used around the mesh with 20 on each flat section. The boundary conditions on the crack plane are shown in figure 11. In regions AB and CD tractions are applied of equal magnitude but opposite sign to those existing in the uncracked ring and the elements are permitted free displacement in the hoop direction. In regions BC and DE no tractions were applied and the elements were permitted no displacement normal to the crack plane (hoop direction). On the uncracked side no tractions were applied and the nodes were held at zero displacement in the hoop direction All other nodes were completely free.

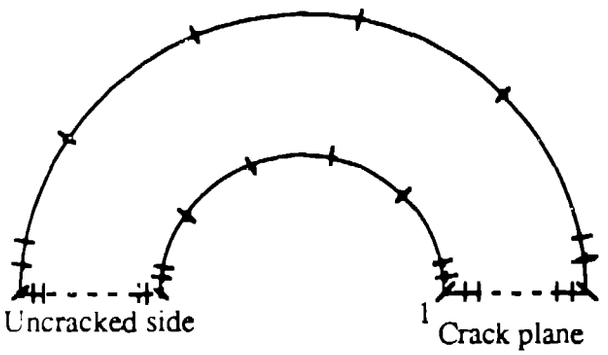

Figure 10: Boundary element mesh

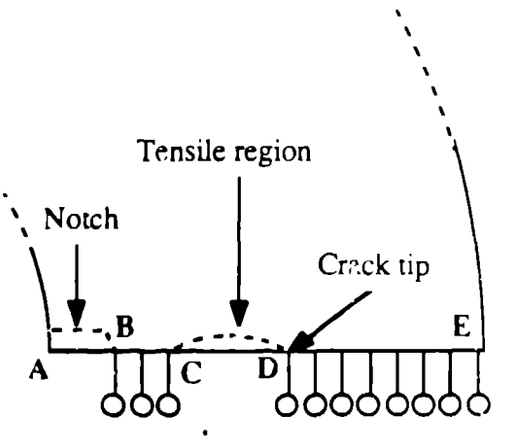

Figure 11: Boundary conditions

In the first analysis the BIE program predicted some overlap of the crack plane to the left of point C (corresponding to R=7.5 at the limit of the compressive hoop stress) in figure 9. When the crack face is shut the solution must not predict overlap of the crack face. Since the contact area was not known in advance, an iterative approach was adopted [9] and the reversed stress distribution was extended backwards to R=5.9mm. Physically this corresponds to the tensile stress holding the crack open at the end of the compressive zone. The crack tip (point D in figure 11) corresponded to R=16.3. The BIE prediction of the redistributed stress is plotted with the measured values in figure 13.

On the uncracked side even when the effect of reversing the stress over the whole length of the longest crack is considered the predicted change to the stresses are less than 15MPa. This is in accordance with the experimental measurements in which no change was observed on the uncracked side, even for the longest crack length.

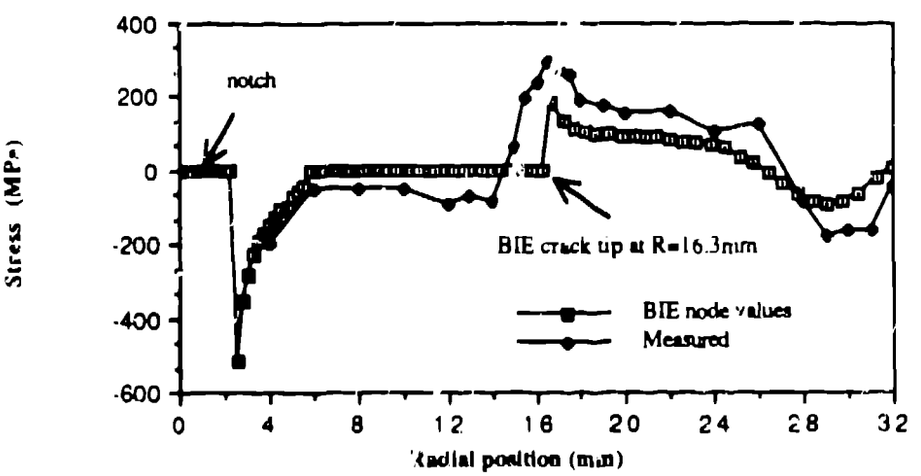

Figure 12: Crack side hoop stress and BIE prediction (A/W = 0.5)

6. Discussion

The BIE analysis was limited by the coarse mesh size and the limited spatial resolution of the measurements. However when the crack tip is assumed to be at R=16.3mm and the crack face is drawn open to R=5.9mm qualitative agreement between the measured results and the BIE predictions is achieved. In figure 12 the first node beyond point D is 0.5mm away. Refinement of the mesh to give the values closer to point D would predict larger tensile stresses which would improve the agreement with the observed data. However, there is considerable discrepancy in the position of the crack tip. The hoop stress results imply that the crack tip lies at or near R=14.5mm since the crack cannot support a tensile stress. However this is shorter than the optical assessment of 16mm. The BIE prediction gives nodal values and strictly some account of the finite size of the sampling volume should be made. Taking the finite sampling volume of the neutron technique into account would improve the agreement between the BIE prediction and the measured values.

In the BIE prediction the stress in the originally tensile region along the crack plane is negated to leave zero stress. This does not account for the constant compressive hoop stress which exists along the crack plane behind the crack tip. Its origin is unclear but may be associated with the plastic wake produced by the passage of the crack.

7. Conclusions

Propagation of fatigue cracks through up to half the wall thickness of autofrettaged specimens has negligible effect on the stress distribution on the opposite uncracked sides. Cracks which remain in the originally compressive region of an autofrettaged ring ring do not modify the residual stresses except due to the artificially introduced notch. However once a crack is propagated into the tensile region distinctive changes occur as the stress redistributes. When a crack had propagated through 8mm of the tensile region the tensile stress ahead of the crack tip increased and reached a maximum of 300MPa which is 3 times the value in an uncracked ring. In the same specimen a constant compressive hoop stress of -80MPa was observed over much of the crack plane except near the bore where the compressive stress was increased due to the removal of the notch material.

The redistribution caused by the longest crack has been addressed using a BIE and superposition approach. The effects of the stress relieved by the crack were calculated and combined with the uncracked stress distribution using the principle of superposition. Qualitative agreement was achieved between the predicted and measured values. The simple analysis fails to account for the compressive shoulder along the crack plane and uncertainty in the spatial resolution of the experimental measurements precluded more detailed attempts to model the stress distributions.

8. References

[1] Stacey, A. & Webster, G.A. "Fatigue crack growth in autofrettaged thick walled high pressure tube material, "High pressure in science and technology, 1984, Mat. res. soc.symp.proc, Part III, Vol. 22, 215-219.

[2] Stacey, A., MacGillivray, H.J., Webster, G.A., Webster, P.J. & Ziebeck, K.R.A. "Measurement of residual stresses by neutron diffraction", Journal of strain analysis, 1985a, Vol. 20, No 2, 93-100.

[3] Pintschovius, L., Macherauch, E., & Scholtes, B.' "Determination of residual stresses in autofrettaged steel tubes by neutron and X-ray diffraction". Proceedings of the

international conference on residual stresses, 1986, Garmisch-Partenkirchen (FRG), 159-165.
[4] Sorem,J.R., Shadley, J.R. & Rybicki, E.F., "Experimental method for determining through thickness residual stresses in thin walled pipes and tubes without inside access", Strain, February 1990, 7-14.
[5] Allen, A.J , Hutchings, M.T., Windsor, C.G. & Andreani, C. "Neutron diffraction methods for the study of residual stress fields", Advances in physics, 1985, Vol. 34, No4, 445-473.
[6] Fenner, R.T.Journal of strain analysis, "The boundary integral equation (boundary element) method in engineering stress analysis", 1983, Vol 18, No4, 199-205
[7] Webster, G.A., Klintworth, G.C. & Stacey, A., "Stress intensity factors for cracked C-shaped and ring type test-pieces", Journal of strain analysis, 1983, Vol 18, No 4, 225-230.
[8] Watson, J.O., Res. Mechanica., "Hermitian cubic boundary elements for plane problems of fracture mechanics", 1982, No4, 23-42.
[9] Becker, A.A. & Plant, R.C.A. "Contact mechanics using the boundary element method", Tribology conference, 1987, Institute of mechanical engineers, C227/87, 975-980